



Morphological Stability during Electrodeposition

II. Additive Effects

Mikko Haataja,^{a,z} David J. Srolovitz,^a and Andrew B. Bocarsly^{b,*}

^aPrinceton Materials Institute and Department of Mechanical and Aerospace Engineering and ^bDepartment of Chemistry, Princeton University, Princeton, New Jersey 08544, USA

Common experience shows that electrodeposited (ED) metallic films exhibit rough surfaces unless the electrochemical bath contains small quantities of molecular additives. We develop a formalism for describing the effects of additives on surface morphology evolution, which builds on that in a companion paper for the additive-free case. We demonstrate that the additives suppress the morphological instability that leads to roughening by preferentially accumulating near surface protrusions and blocking growth sites. Our chemically based model shows that additives which readily adsorb onto the surface and have a strong tendency to complex with the metal cations reduce the driving force for the instability and thus enhance leveling. Furthermore, polar additives provide an additional stabilizing effect, in accord with experimental observations. It is also shown that linearly stable growth can be achieved over a wide range of deposition flux at sufficiently large additive bulk concentrations. We predict the ED conditions necessary for growing flat films and demonstrate that these are in good agreement with experimental observations.

© 2003 The Electrochemical Society. [DOI: 10.1149/1.1602456] All rights reserved.

Manuscript submitted January 28, 2003; revised manuscript received April 7, 2003. Available electronically August 18, 2003.

Extensive experience shows^{1,2} that the properties of electrodeposited (ED) metallic films can be effectively controlled by introducing small quantities of additives into the electrochemical bath. For example, morphological instabilities during deposition commonly produce poor quality films with rough surfaces³⁻⁷ in the absence of additives. Addition of even small quantities of additives can drastically decrease the amplitude of the surface roughness as well as increase the characteristic wavelength of the roughness.⁷ In addition to controlling the large-scale roughness (leveling), additives have been used to control crystallographic texture and grain size of ED films. The goal of the present paper is to provide a formalism which can be used to evaluate proposed mechanisms for surface leveling by the introduction of additives into the electrochemical baths. We apply this formalism to explicitly evaluate the effects of complex formation between cations and additives, additive dipole moments, surface segregation, and additive incorporation into the growing electrodeposit.

Typically, additives consist of organic compounds or small inorganic species that can act as ligands with respect to the metal being deposited. The ionic nature of the additive along with the exact mode of ligation is extremely variable. Commonly employed additives can be organic (*e.g.*, thiourea, CH₄N₂S in nickel plating baths) or inorganic (*e.g.*, potassium nitrate, KNO₃ in silver plating baths), ionic (*e.g.*, sodium sulfocyanate, NaSCN in silver electrodeposition), or nonionic, polar (*e.g.*, naphthoquinone, C₁₀H₆O₂ in lead electrorefining) or nonpolar (*e.g.*, anthraquinone, C₁₄H₉NO₂ in lead electrorefining).² This suggests that the leveling effect of the additives depends on only a few key physical characteristics.

While there are many commercial levelers, a complete understanding of their effects and the physical and chemical mechanisms that allow these molecules to effectively reduce the roughness of films remains elusive. This is in contrast with the emerging understanding of the role of additives in vapor phase deposition; *e.g.*, the surfactant effect in semiconductor growth (see Ref. 8 and references cited therein). In Part I⁹ we presented a formalism that provides quantitative predictions for the evolution of the surface morphology in the absence of additives. In this paper we extend the formalism of Part I to the case where ED occurs in the presence of additives. We present a physically and chemically motivated model for ED with additives, then investigate the influence of the additives on the morphological evolution and stability of surfaces during ED. A brief account of this work has appeared in Ref. 10.

Morphology evolution in the presence of additives has been previously addressed through both experiments^{2,7} and theory.¹¹⁻¹⁴ Qualitatively, there is some experimental evidence suggesting that polar additives or additives which tend to form complexes with the metal cations lead to more effective leveling.^{1,2} An experimental study of the growth of copper films from a copper sulfate bath produced increasingly rough surfaces during growth in the absence of additives, while adding thiourea led to smoother films.⁷ Increases in thiourea concentration led to smoother films and longer wavelength roughness. A range of thiourea concentration exists for which the growth front remains essentially flat. We argue that this is attributable to the complete suppression of growth instability for additive concentrations larger than a critical value.

Several models have been proposed to explain the leveling effects of additives. They all assume that the additives adsorb onto the growing surface and interfere with the deposition process through a specific mechanism, such as blocking the surface growth sites,^{1,2,11} the leveling effect results from preferential growth at surface depressions instead of protrusions. Madore *et al.*¹¹ introduced a continuum model which included the blocking effect of charged additives as well as additive reduction at the electrode, coupled to diffusive transport of the additives to the surface. They found that the leveling effect of additives is controlled by the ratio of the additive diffusivity to the rate of additive consumption at the cathode. Georgiadou *et al.*¹² studied the evolution of film morphology during ED of copper in microtrenches by employing a model where the additive suppresses metal deposition and is consumed by an electrochemical reaction. By numerically solving the full nonlinear moving boundary problem they demonstrated that the additives promote void-free filling of trenches. Similarly, Cao *et al.*¹³ numerically solved a model in which the adsorption of additives locally inhibits deposition and showed that this leads to effective leveling and void-free filling of trenches. Recently, Pricer *et al.*¹⁴ introduced a coupled Monte-Carlo/continuum approach for studying the effect of a blocking additive in copper ED in rectangular trenches. Finally, Josell *et al.*^{15,16} have recently introduced an accelerator-additive model which quantitatively explains superconformal ED in submicrometer features.

While the aforementioned theoretical approaches have successfully explained some of the experimental results, they have neglected several common experimental observations and have based their models on an oversimplified picture of transport in the electrolyte. For example, effective additives are known to ligand to the electroactive metal ions, forming complexes in solution. The additives alone or in a complex can produce neutral species which interact with the electric field through strong molecular dipole mo-

* Electrochemical Society Active Member.

^z E-mail: mhaataja@princeton.edu

ments. We consider several types of additive/metal ion interactions and explicitly account for metal cation and additive drift in the electric field within electrolytes that are not fully supported. Including the effects of spectator ions allows us to interpolate between the limiting cases of fully supported (purely diffusive transport) and unsupported electrolytes. The resultant linear stability theory allows us to examine the interplay between additive and metal ion transport, drift, and diffusive transport and make predictions about the resulting morphology in terms of the external control parameters (e.g., additive bulk concentration, spectator ion concentration, deposition flux) and the chemical properties of the metal cations and additives (e.g., charge, dipole moment, heat of segregation, and complex formation).

In the next section we very briefly review the relevant aspects of the formalism and the results on growth instabilities in the absence of additives from the companion paper, Part I.⁹ We then describe several physical and chemical models for the mechanisms by which the additives influence the deposition process. Then we perform a self-consistent, uniform steady-state analysis of ED in the presence of additives (including the concentration and electrostatic fields). Morphology evolution is analyzed using perturbation theory, where we linearize around the uniform steady-state result. The resultant predictions for the wavelength and growth rate of the roughness as a function of chemical and deposition parameters are collected in the form of a stability map, which shows under which conditions the surface instability can be entirely suppressed. Finally, we compare our predictions with experimental observations.

Model for Electrodeposition in the Absence of Additives

Formalism.—We briefly review the relevant aspects of the morphology evolution formalism put forth in Part I. The number density for each ionic species obeys a continuity equation

$$\frac{\partial C_i}{\partial t} + \nabla \cdot \mathbf{j}_i = 0 \quad [1]$$

where $i = C, A, XC, XA$ denotes the metal cations, anions, spectator cations, and spectator anions, respectively. The ion fluxes $\mathbf{j}_i(\mathbf{r})$ follow from

$$\mathbf{j}_i(\mathbf{r}) = -D_i \nabla C_i - \frac{q_i e D_i C_i}{k_B T} \nabla \phi \quad [2]$$

where D_i denotes the diffusivity and ϕ is the electrostatic potential. ϕ is determined from the Poisson equation¹⁷

$$\nabla^2 \phi = -\frac{e}{\hat{\epsilon}} \sum_i q_i C_i(\mathbf{r}) \quad [3]$$

where $\hat{\epsilon}$ denotes the constant local permittivity of the ionic solution.

We consider a rectangular system of dimensions $L_x \times L_z = W \times L$, where W denotes the linear dimension (width) of the planar surface and L denotes the thickness of the mass-transfer layer over which the concentrations vary. Beyond L the concentrations of all species are very nearly constant. Periodic boundary conditions are employed in the x direction, and the boundary conditions in the z direction become $C_C(x, L) = C_A(x, L) = C_0$, $C_{XC}(x, L) = C_{XA}(x, L) = C_1$, and $\phi(x, L) = 0$. At the growing surface $\phi(x, 0) = V_{\text{ext}}$, and the ion fluxes $i = (A, XC, XA)$ vanish as these species do not codeposit: $j_i = -\mathbf{j}_i \cdot \hat{n} = 0$, where \hat{n} is the surface normal (pointing into the bath). The magnitude of the local metal cation flux onto the growing surface j_C (taken to be positive for a growing film) is given by the Butler-Volmer (B-V) equation

$$j_C = -\mathbf{j}_C \cdot \hat{n} = j_0 \left(\frac{C_C}{C_0} e^{\alpha_1 F \eta / RT} - e^{-\alpha_2 F \eta / RT} \right) \quad [4]$$

where F and R are the Faraday's and gas constants, and (α_1, α_2) denote the so-called symmetry factors related to the potential barrier for metal cation reduction.¹⁸ The overpotential η is given by¹⁹

$$\eta = V_{\text{eq}} - V_{\text{ext}} + \frac{RT}{F} \ln \left(\frac{C_C}{C_C^{\text{eq}}} \right) + \frac{\Omega \gamma \kappa}{F q_C} \quad [5]$$

The equilibrium potential of the metal-solution interface is V_{eq} , and varying the external electrode potential V_{ext} away from V_{eq} leads to either deposition ($\eta > 0$) or dissolution ($\eta < 0$). The third term in Eq. 5 accounts for the metal cation concentration dependence of V_{eq} , and the last term describes the effects of surface curvature κ and surface tension γ , *i.e.*, the Gibbs-Thomson effect. The quantity $q_C e j_0$ denotes the exchange current density, and Ω denotes the atomic volume of the metal in the deposit. Finally, the local growth velocity in the normal direction \hat{n} , v_n , follows from the mass-balance relation $v_n = -\Omega \mathbf{j}_C \cdot \hat{n}$.

Morphology evolution.—In Part I we introduced a physically motivated continuum model for the morphological stability of surfaces during ED in the absence of additives. The model explicitly accounts for the electric field in the electrolyte, the metal cations and anions, and any additional ions from a supporting electrolyte. By explicitly solving the steady-state equations for a planar growth front, we demonstrated that the model naturally gives rise to the Gouy-Chapman (G-C) boundary layer and that increasing the concentration of the spectator ions leads to a rapid decrease in the magnitude of the electric field in the bulk. In this limit the metal cation transport is dominated by diffusion in the concentration gradient, as expected. A first understanding of the morphology evolution was obtained by carrying out a perturbation analysis in the surface profile. In agreement with previous stability analysis,²⁰⁻²⁵ the surface was shown always to be linearly unstable against perturbations with a sufficiently large wavelength for any finite external deposition flux. This result holds for both unsupported and fully supported baths and can be understood as follows. Consider a small perturbation to the planar surface. Because C_C increases away from the growing surface, the metal cation concentration C_C is larger (smaller) near protrusions (depressions) than near the flat surface. In the absence of surface tension an increase in C_C leads to a larger metal cation flux via the B-V equation, Eq. 4. The larger metal cation flux leads to an increase in v_n and hence, to faster (slower) growth at a protrusion (depression). This positive feedback leads to unstable growth of the perturbations. Capillarity, however, effectively suppresses perturbations on small scales, and these two competing effects (deposition and capillarity) set the lateral scale of the surface roughness observed in experiment. In particular, increasing the deposition flux makes the surface rough on smaller scales and leads to faster roughening. Interestingly, for a fixed deposition flux j the system without the supporting electrolyte was found to be more stable than one with a supporting electrolyte, in agreement with previous studies.²² This was shown to be a consequence of the increasing local metal cation concentration gradient as more spectator ions are added into the bath.

Models for Additive Effects in Electrodeposition

We now turn to the description of additives within the framework introduced in Part I. Qualitatively, there are three main questions that must be considered in assessing the role of additives in ED: (i) how do they interact with the ions in the bulk, (ii) how do they get to the surface, and (iii) once on the surface, how do they modify the deposition of the metal cations. It has been suggested that a metal cation and an additive molecule can form a complex in the bulk solution;^{1,2} in particular, it has been noted that increasing the tendency of metal ions to form complexes with the additives correlates with their susceptibility to the effect of additives.¹ The transport of the additives to the surface is usually assumed to be

diffusion-limited,^{2,7,14} although it is conceivable that some of the additives are brought onto the surface through the motion of the metal cations as a part of a complex.

Several models have been proposed to explain the leveling effects of additives, the most popular of which are (i) blocking the surface, (ii) changes in the boundary layer potential, and (iii) ion bridging.^{1,2} The first mechanism, also known as the “dirt” mechanism, is attributed to the tendency of the additive molecules to adsorb onto the surface and interfere with either the attachment of metal cations or their diffusion along the surface to preferential growth sites. This type of additive causes a decrease in the rate of the electrode reaction at fixed potential. The leveling effect of such additives can be understood by considering the additive concentration around a protrusion: if the protrusion “collects” more additives than do depressions (e.g., due to an additive concentration gradient), it tends to grow more slowly than the depressions, implying leveling.^{2,7,14} The second mechanism is based on the idea that the reduction reaction does not necessarily have to occur at the surface but can take place anywhere within the G-C boundary layer.² Therefore, any foreign ions or neutral molecules which adsorb onto the surface modify the potential within the G-C boundary layer and thus influence the deposition rate. Finally, the additives may increase the rate of reduction;² this could apply to additives which bond to the surface and mediate the charge transfer between the metal cation and the deposit (ion bridging).

It is noteworthy that the effect of a particular additive species can be a combination of all these mechanisms. Furthermore, there is some evidence that the leveling is brought about through the interaction between reaction products of the additive at the surface and the growing deposit.² Finally, in some cases the growth of a level and bright deposit requires the simultaneous use of multiple types of additives. Such synergistic effects are not considered here.

In light of this discussion it is clear that unraveling the underlying mechanisms for the leveling effect of a given additive molecular species is a daunting task. Therefore, the goal of the present work on additive effects is by necessity somewhat more limited, namely, to construct a minimal model for additive effects, to quantify the role of different interactions in the morphology evolution of the surface, and finally, to relate this to leveling. In particular, we consider additives which (i) form complexes with the metal cations, (ii) interact with the electric field via a dipole moment, and (iii) interfere with the deposition process by blocking surface growth sites. Although some of the microscopic details are necessarily ignored in this approach, many of the common properties of additives are accounted for. This approach provides a means to assess the importance of different types of interactions and therefore provides a guide for the development of additives.

Coupling between the additives and the deposition process.—Complex formation.—We assume that complex formation between the additives and the metal cations is local and pairwise. That is, we model complex formation between cations and additive in a small volume of space as proportional to the product of the concentration of each in this volume. To obtain the contribution of complex formation to the total Helmholtz free energy, we add the contributions of each local volume element as

$$F_C = - \int \psi C_C(\mathbf{r}) C_I(\mathbf{r}) d\mathbf{r} \quad [6]$$

This type of expression is commonly used in statistical mechanics treatments of solution theory.²⁶ In this equation ψ is a parameter which characterizes the strength of the local attractive interaction between the additives and the metal cations. A simple relation between the heat of complex formation ΔQ_1 per additive molecule and the parameter ψ can be established by assuming that one additive molecule interacts with a single metal cation: $\psi = \Delta Q_1 / C_0$. In this model any inhomogeneities in the metal cation concentration are accompanied by a variation in the additive concentration $C_I(\mathbf{r})$.

Equation 6 accurately describes the interaction between the additives and the metal cations through complex formation, given that the complexes are relatively weakly bound, which implies that $\Delta Q_1 \approx k_B T$.

Polar additives.—There is experimental evidence² that polarity of the additives enhances the stability of the growing surface. It has been observed in lead electrorefining that naphthoquinone, which has a molecular dipole moment, is a very good leveler, while a chemically similar complex molecule anthraquinone (with very small molecular dipole moment) has a very small leveling effect. Hence, it has been hypothesized² that the leveling capacity of naphthoquinone can be attributed to the finite molecular dipole moment which allows the additives to interact with the inhomogeneous electric field at the metal/solution interface.

The energy of a dipole in an electric field is simply the dot product of the dipole moment vector and the local electric field.¹⁷ The total interaction energy of the dipole moment on the additives and the electric field F_E is proportional to the local concentration of dipoles (additives) and the local electric field summed over all small volume elements

$$F_E = - \int C_I \mathbf{p} \cdot \nabla \phi d\mathbf{r} \approx - \int_r C_I |\mathbf{p}| |\nabla \phi| d\mathbf{r} = - \int_r C_I p |\nabla \phi| d\mathbf{r} \quad [7]$$

where \mathbf{p} is the molecular dipole vector of the additives, and the last two equalities assume that the molecules quickly orient with their dipoles along the field. Note that this coupling enhances the concentration of additives in regions where the magnitude of the electric field is large.

Transport equations and fluxes.—Based on the additional interaction terms introduced we rewrite the metal cation flux as

$$\mathbf{j}_C(\mathbf{r}) = -D_C \nabla C_C - \frac{qeD_C C_C}{k_B T} \nabla \phi + \frac{D_C \psi C_C}{k_B T} \nabla C_I \quad [8]$$

The last term is due to the coupling between the additives and the metal cations, as described by Eq. 6. Because the anions are assumed not to form complexes with the additives their flux is still written as

$$\mathbf{j}_A(\mathbf{r}) = -D_A \nabla C_A + \frac{qeD_A C_A}{k_B T} \nabla \phi \quad [9]$$

Finally, the additive flux reads

$$\mathbf{j}_I(\mathbf{r}) = -D_I \nabla C_I + \frac{D_I p C_I}{k_B T} \nabla |\nabla \phi| + \frac{D_I \psi C_I}{k_B T} \nabla C_C \quad [10]$$

The additive flux has contributions from diffusion, gradients in the electric field if the molecules are polar ($p \neq 0$), adsorption to the surface, and complex formation with the metal cations. Diffusion tends to smooth out the inhomogeneities in the concentration profile, whereas the additives tend to accumulate in regions of large electric field gradients (because the additives are polar), large metal cation concentration, or both.

Additives and surface site blocking.—We incorporate the effect of additives in blocking potential surface growth sites by adopting a modified B-V equation for the local metal cation flux j_C which satisfies

$$j_C = \left(D_C \nabla C_C + \frac{D_C q e C_C}{k_B T} \nabla \phi - \frac{D_C \psi C_C}{k_B T} \nabla C_I \right) \times \hat{n} = j_0 (1 - \theta_I) \left(\frac{C_C}{C_0} e^{\alpha_1 F \eta / RT} - e^{-\alpha_2 F \eta / RT} \right) \quad [11]$$

where θ_1 denotes the additive surface coverage. We describe the surface coverage using a Langmuir isotherm

$$\theta_1 = \frac{KC_1}{1 + KC_1} \quad [12]$$

where the adsorption equilibrium constant $K = \exp(\Delta Q/k_B T)$ and ΔQ denotes the heat of adsorption. The tendency of the additives to locally block some of the available growth sites on the surface (thus leading to slower deposition rates for high local additive coverage) is phenomenologically incorporated by the multiplicative term $(1 - \theta_1)$ in the local flux. In particular, we assume that a sufficiently high additive concentration can lead to a total saturation of the growth sites on the surface, and hence to a suppression of deposition. This model qualitatively captures the salient features of the interaction between additives and the metal cations at the growth surface.

We also consider the possibility that the additives on the surface may be incorporated into the growing film by codeposition along with the metal cations. This codeposition is modeled by imposing a dimensionless additive flux at the surface which is proportional to the local metal cation flux: $j_1 = \chi C_1^\infty j$, where the proportionality constant χ describes the extent of codeposition and C_1^∞ denotes the dimensionless additive bulk concentration. While this admittedly constitutes an oversimplification of the true surface physics, it is consistent with experimental observations and allows us to assess the importance of codeposition on the growth of ED films, of which little is generally known. Note that $\chi = 1$ implies that metal cations and additives are incorporated into the growing deposit in proportions given by their bulk concentrations.

It is noteworthy that a finite dipole moment effectively increases the equilibrium constant K as the polar additives are attracted to the surface by the large electric field strengths. Unfortunately, it is generally not easy to estimate the contribution of this interaction to K quantitatively because it depends on the detailed atomic structure of the surface and the structure of the additive in question. However, as a simple estimate we consider a typical electric field strength of ~ 0.3 V/nm at the interface and a typical dipole moment of $\sim 5e$ Å for a polar molecular species, the product of which is the dipole moment contribution to ΔQ . Using these values we find that this contribution is ~ 0.125 eV, which is larger than $k_B T$ by a factor of order 3 or 4 at room temperature. This translates into a change in the value of K by a factor of nearly 25, as compared with its value if no dipole moment were present. A dipole moment on the additives may also play a minor role on the metal cation-additive complex formation. However, in order to assess the significance of the aforementioned interactions on the growth front stability, we treat K , p , and ψ as independent parameters in the remainder of the paper.

Steady-state properties.—We again examine the steady-state properties of the model as a prerequisite to the morphology analysis. In steady state the metal cation flux is constant across the length of the cell, while the anion and spectator ion fluxes vanish, respectively. Therefore, upon measuring all lengths in units of the mass-transfer layer thickness L (and thus all wavenumbers in units of $1/L$), time in units of diffusion time L^2/D_C , ionic and additive concentrations in units of the bulk metal cation concentration C_0 , electric potential in units of the equilibrium voltage V_{eq} , and fluxes in units of the diffusion-limited flux $D_C C_0/L$ as employed in Part I, we may write the new dimensionless steady-state equations as

$$\frac{d}{dz} C_C + \beta C_C \frac{d}{dz} \phi - Y C_C \frac{d}{dz} C_1 = j$$

$$\frac{d}{dz} C_A - \beta C_A \frac{d}{dz} \phi = 0$$

$$\frac{d}{dz} C_{XC} + \beta C_{XC} \frac{d}{dz} \phi = 0$$

$$\frac{d}{dz} C_{XA} - \beta C_{XA} \frac{d}{dz} \phi = 0$$

$$\frac{d}{dz} C_1 - \Delta C_1 \frac{d}{dz} \left| \frac{d}{dz} \phi \right| - Y C_1 \frac{d}{dz} C_C = D_1^C \chi C_1^\infty j$$

$$\epsilon^2 \frac{d^2}{dz^2} \phi = -(C_C + C_{XC} - C_A - C_{XA}) \quad [13]$$

where $D_1^C \equiv D_C/D_1$, and where we have used two important dimensionless parameters $Y \equiv \psi C_0/(k_B T) = \Delta Q_1/(k_B T) = \ln K_C$ and $\Delta \equiv V_{eq} p/(k_B T L)$ in the additive flux. Y describes the interaction strength for complex formation and Δ describes the interaction strength between the additives and the inhomogeneous electric fields through the finite molecular dipole moment. Furthermore, K_C denotes the equilibrium constant for complex formation between the additives and the metal cations. In the subsequent calculations we employ $L = 4 \times 10^{-4}$ m, appropriate for free convection electroplating conditions.

Written in a dimensionless form, it can be inferred from the metal cation steady-state equation in Eq. 13 that the term $Y C_C dC_1/dz$, arising from complex formation, is typically very small in magnitude ($\sim 10^{-6}$) compared to the diffusion and drift terms (~ 1), because the bulk additive concentration $C_1^\infty \sim 10^{-6} \times C_0$. Therefore, we may drop the last term in the metal cation flux to a very good approximation. Note, however, that the complexing term cannot be neglected in the additive flux and is thus retained in the following analysis. Because the additives now affect the metal cation concentration only through the modified B-V boundary condition, the steady-state solutions for C_C and ϕ are exactly as given in Part I in the absence of additives

$$C_C = (1 + C_1) \exp(\beta \phi) - C_1 \exp(-\beta \phi) - \epsilon^2 \frac{d^2 \phi}{dz^2} \quad [14]$$

where

$$\begin{aligned} \phi(z, j) = & - \left[\frac{1}{\beta \phi^*} \ln \left(1 - \frac{j}{2 + 2C_1} \right) - 1 \right] \\ & \times \frac{4}{\beta} \tanh^{-1} \left(e^{-\sqrt{2\beta(1+C_1)}z/\epsilon} \tanh \frac{\beta \phi^*}{4} \right) \\ & + \frac{1}{\beta} \ln \left(1 - \frac{j}{2 + 2C_1} + \frac{jz}{2 + 2C_1} \right) \end{aligned} \quad [15]$$

and $\phi^* \equiv V_{ext}/V_{eq}$. This solution is accurate to lowest order in ϵ everywhere and to lowest order in $j/(1 + C_1)$ within the boundary layer $0 \leq z \leq \epsilon$ and to all orders in j in the bulk. Similarly, the steady-state solutions for C_A , C_{XA} , C_{XC} , and C_1 are simply $C_A = e^{\beta \phi}$, $C_{XC} = C_1 e^{-\beta \phi}$, and $C_{XA} = C_1 e^{\beta \phi}$, and

$$C_1 \approx C_1^\infty e^{(Y C_C + \Delta |d\phi/dz|)} (1 - D_1^C \chi j + D_1^C \chi j z) \quad [16]$$

appropriate for $\chi \ll 1$. We note that the additive concentration at the surface is given by (cf. Eq. 16)

$$C_1(0) = C_1^\infty e^{(Y C_C(0) + \Delta |d\phi(0)/dz|)} (1 - D_1^C \chi j) \quad [17]$$

It is noteworthy that the large electric fields in the boundary layer effectively attract polar additive particles.

In order to get a better understanding of the effects of the various parameters in the additive concentration profile C_1 , we plot some representative profiles in steady state in the absence of spectator ions in Fig. 1. In particular, Fig. 1a shows the equilibrium ($j = 0$) concentration profiles for several values of the interaction parameter Y that describes the strength of complex formation. Notice how an

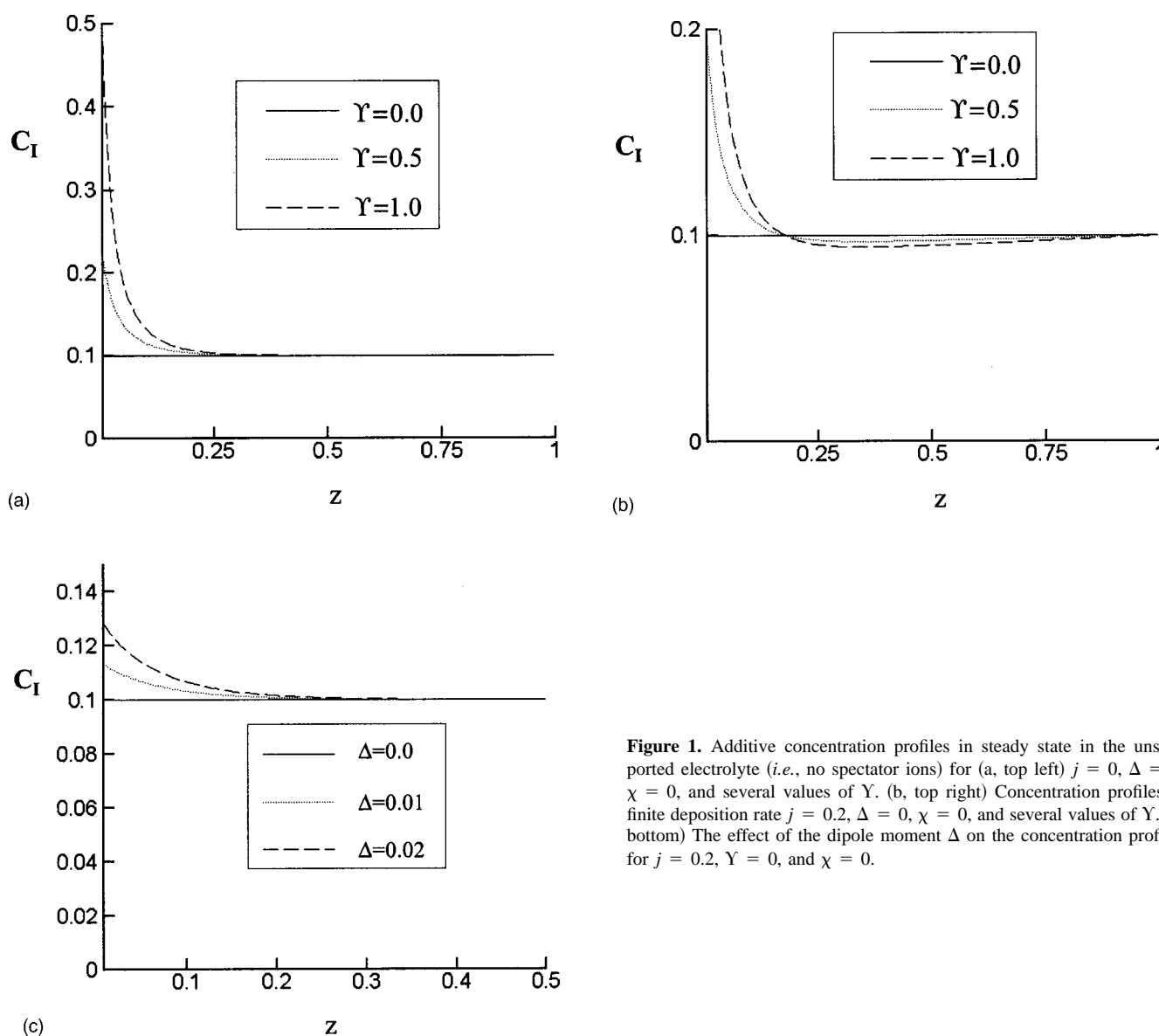


Figure 1. Additive concentration profiles in steady state in the unsupported electrolyte (*i.e.*, no spectator ions) for (a, top left) $j = 0$, $\Delta = 0$, $\chi = 0$, and several values of Y . (b, top right) Concentration profiles at finite deposition rate $j = 0.2$, $\Delta = 0$, $\chi = 0$, and several values of Y . (c, bottom) The effect of the dipole moment Δ on the concentration profiles for $j = 0.2$, $Y = 0$, and $\chi = 0$.

increase in the metal cation concentration in the vicinity of the boundary layer leads to a corresponding increase in C_I due to this attractive interaction. Additionally, the additive concentration attains a constant value away from the boundary layer. Upon applying an external deposition flux, the additive concentration profile is influenced by the metal cation concentration gradient in the bulk, as shown in Fig. 1b for $j = 0.2$, $\Delta = 0$, $\chi = 0$, and several values of Y . In particular, an additive concentration gradient in the bulk develops in steady state due to the interaction between the metal cations and additives. Finally, in Fig. 1c we plot the additive concentration profiles in the absence of complex formation for $j = 0.2$, $Y = 0$, $\chi = 0$, and several values of the parameter Δ which describes the coupling between the electric fields and the polar additives. Note the accumulation of additives within the boundary layer as a consequence of their interaction with the electric field.

Linear stability analysis: Additive effects.—Next we apply the linear stability analysis to determine how the surface evolves during ED in an electrolyte containing additives. The analysis follows the procedure described in Part I in the absence of additives. In the fully

supported electrolyte case the analysis is carried out analytically and is valid for all values of the deposition flux j , while in the partially supported electrolyte case the analysis is carried out as a perturbation expansion in the flux j , as outlined in Appendix B of Part I in the absence of additives.

Physically, the additives occupy surface sites where metal cations can attach, thus slowing growth. Therefore, if protrusions collect more additives than depressions they grow more slowly, hence favoring the growth of smooth surfaces.^{7,14,18} Increased additive concentrations occur where the additive flux to the surface is greatest. This flux is controlled by (i) additive-metal cation complexing (represented by Y) in which the metal cations drag the additives to the growth front during deposition, (ii) interactions between the polar additives and the inhomogeneous electric field associated with the surface perturbation, and by (iii) additive codeposition (represented by χ) which gives rise to an additive concentration gradient. The linear stability analysis shows that the perturbation growth rate in the presence of additives $\omega(k)$ in a fully supported electrolyte is given by

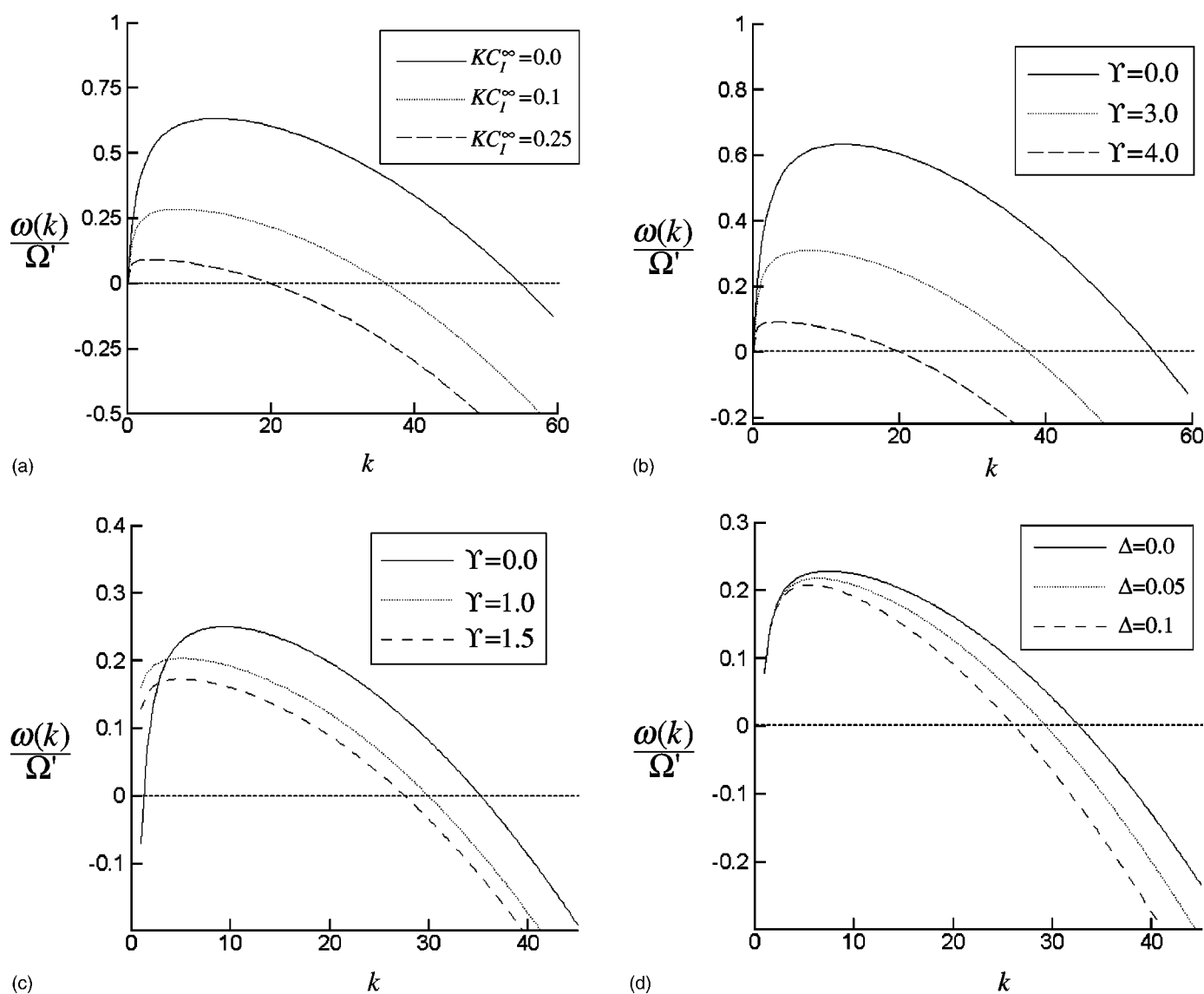


Figure 2. Linear dispersion relation $\omega(k)/\Omega'$ vs. k for a fully supported electrolyte with (a, top left) $j = 0.5$, $Y = 4.0$, $\chi = 0.0$, $\alpha_1 = 0.5$, and $\hat{\gamma} = 0.001$ and several values of KC_1^∞ and (b, top right) $j = 0.5$, $KC_1^\infty = 0.25$, $\chi = 0.0$, $\alpha_1 = 0.5$, and $\hat{\gamma} = 0.001$ and several values of the parameter Y describing complex formation. Linear dispersion relation $\omega(k)/\Omega'$ vs. k for an unsupported electrolyte for (c, bottom left) $j = 0.5$, $KC_1^\infty = 0.5$, $\chi = 0.0$, $\alpha_1 = 0.5$, and $\hat{\gamma} = 0.001$ and several values of the parameter Y and (d, bottom right) $j = 0.5$, $KC_1^\infty = 0.25$, $\chi = 0.0$, $\alpha_1 = 0.5$, $\hat{\gamma} = 0.001$, and $Y = 1.0$, and several values of the parameter Δ which describes the dipole moment of the additives.

$$\frac{\omega(k)}{\Omega'} = \frac{jk \left[\frac{j_{\text{eff}}(1 + \alpha_1)}{(1 - j_{\text{eff}})} - \hat{\gamma}\alpha_1 k^2 \right]}{\left[\frac{j(1 + \alpha_1)}{(1 - j)} - j\Gamma Y(1 - D_1^C \chi j) + k \right]} \quad [18]$$

where the effective current $j_{\text{eff}}(1 + \alpha_1)/(1 - j_{\text{eff}}) \equiv j(1 + \alpha_1)/(1 - j) - \Gamma(jY + D_1^C \chi j - j^2 D_1^C \chi Y)$, and the additive effects are conveniently expressed by Γ as

$$\Gamma \equiv \frac{KC_1^\infty e^{Y(1-j)}}{1 + KC_1^\infty e^{Y(1-j)}(1 - D_1^C \chi j)} \quad [19]$$

Qualitatively, Eq. 18 is very similar to the corresponding result in the absence of additives, Eq. 17 in Part I. In particular, the growth rate $\omega(k)$ is positive for small k and becomes negative for $k > k_0$, implying stability on scales $\ell < \ell_s \equiv 2\pi/k_0$, where ℓ_s denotes the stabilization length. Equation 18 has a very appealing

physical interpretation. The presence of additives gives rise to an effective flux j_{eff} , the magnitude of which depends on the additive bulk concentration C_1^∞ , the strength of complex formation Y , the degree of codeposition χ , and the susceptibility to segregate onto the surface of the growing film, described by the equilibrium constant K . Because j_{eff} is always less than j , the metal cation flux driven instability is reduced by the presence of the additives. This follows from the key observation in Part I, *i.e.*, that the morphological instability in the absence of additives is due to the finite deposition flux j , and decreasing j makes the surface smoother.

In Fig. 2a we plot $\omega(k)$ vs. k , several additive concentrations C_1^∞ , and a fixed metal cation deposition flux j . The other parameters were set to $j = 0.6$, $Y = 4.0$, $\chi = 0.0$, $\alpha_1 = 0.5$, and $\hat{\gamma} = 0.001$. Note that increasing C_1^∞ leads to reduced k_{max} and instability growth rates, $\omega(k)$. Thus, increasing the additive concentration increases the range of surface stability (implying leveling) for the same external deposition flux j . Closer examination of Eq. 18 also reveals that increasing the degree of additive codeposition (χ

> 0), the equilibrium additive surface concentration (represented by K), and the degree of coupling Y between additives and metal cations all enhance stability, consistent with experimental observations.² This is illustrated in Fig. 2b, where we show $\omega(k)$ vs. k for several values of the interaction parameter Y with $j = 0.5$, $KC_1^\infty = 0.25$, $\chi = 0.0$, $\alpha_1 = 0.5$, and $\hat{\gamma} = 0.001$. We note that the additives can increase the surface stability even without additive incorporation into the growing film (as clearly seen from this figure).

Let us now explicitly compare our predictions for surface stabilization with existing experimental data. In particular, in Ref. 7 the growth of copper deposits from a copper sulfate bath in the presence of thiourea was studied. For example, employing the current density $J = 200 \text{ A/m}^2$ and cation bulk concentration $C_0 = 0.6 \text{ M}$ from Ref. 7, and employing the reasonable values $D_C \approx 10^{-9} \text{ m}^2/\text{s}$, $\gamma \approx 1.6 \text{ J/m}^2$, $K = 10^6$, $\alpha_1^I = 1$, and $\chi = 0.5$, and experimentally determined value $0.8 < Y < 1.5$,^c appropriate for thiourea-cupric complexes, we find that an additive bulk concentration of 0.025 mM leads to the stabilization length $0.1 \text{ mm} < \ell_s < 0.2 \text{ mm}$, in good quantitative agreement with experimental result of $\ell_s \sim 0.5 \text{ mm}$ in Ref. 7.

It is noteworthy that the parameter Δ which describes the strength of the interaction between the polar additives and the electric field does not explicitly appear in Eq. 18. This is a direct consequence of the fact that for a sufficiently large spectator ion concentration, the electric field is almost completely screened in the bulk, and therefore it is practically unaffected by the surface perturbation. This implies that the electric field around a protrusion is the same as for a flat part of the surface or a depression, and therefore the interaction between the dipole moment on the additives and the perturbed electric field does not modify the additive efficacy in stabilizing the surface in the fully supported electrolyte. Increasing the additive dipole moment effectively increases the equilibrium constant K as the additives are attracted to the surface by the large electric field strengths, and this helps stabilize the surface, as discussed previously. In the partially supported electrolyte case, the polar nature of an additive can play a further stabilizing role, as discussed shortly.

We have also performed a stability analysis for ED in the presence of additives for the case in which the electrolyte is unsupported or only partially supported using the same approach as outlined in the previous section and in Appendix B. Figure 2c shows the perturbation growth rate $\omega(k)/\Omega'$ as a function of wavenumber for the case of the completely unsupported electrolyte ($C_1 = 0$), for $j = 0.5$, $KC_1^\infty = 0.5$, $\chi = 0.0$, $\alpha_1 = 0.5$, $\hat{\gamma} = 0.001$, and several values of Y . As in the fully supported electrolyte case, increasing Y is beneficial for stability. Increasing the bulk additive concentration and the surface coverage of the additives through increasing the equilibrium constant K also increases the surface stability (not shown), as in the fully supported electrolyte case.

A novel feature arises in the unsupported or partially supported electrolyte case when the dipole moment of the additives is finite, as anticipated previously. During deposition, a finite electric field is set up in the bulk; the presence of this field is due to the absence of spectator ions and it persists for small spectator ion concentrations, as shown in Part I. Consider next the nonzero electric field associated with a surface protrusion. Since the growing surface is an equipotential one, it follows that the equipotential lines are crowded together ahead of the protrusion, and the corresponding electric field becomes large (this is shown explicitly in Part I, Appendix B); the opposite is true for a depression. Because the polar additives are attracted to regions of large electric fields, a protrusion collects more additives, which tends to stabilize the surface. These physical arguments are confirmed by calculating the linear stability curves for an

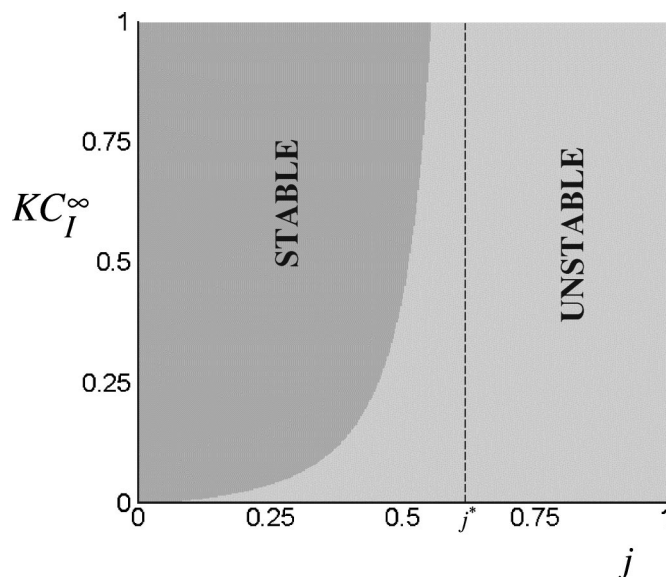


Figure 3. A stability map showing fixed sample dimensions and experimental conditions for which the ED surface is smooth (stable) or rough (unstable) for $Y = 4.0$, $W = 1.0$, $\chi = 0.0$, $\hat{\gamma} = 0.001$, and $\alpha_1 = 0.5$.

unsupported electrolyte with polar additives. The results are shown in Fig. 2d, where we plot $\omega(k)/\Omega'$ for $j = 0.5$, $KC_1^\infty = 0.25$, $\chi = 0.0$, $\alpha_1 = 0.5$, $\hat{\gamma} = 0.001$, and $Y = 1.0$, and several values of the parameter Δ which is related to the dipole moment of the additives. It can be seen that increasing Δ is beneficial for leveling. However, the main additional stabilizing effect of dipolar additives comes from a larger effective equilibrium constant K , as $\Delta \approx 10^{-5}$ for $L \approx 10^{-4} \text{ m}$, appropriate for typical electroplating conditions.

Additive-assisted growth of linearly stable surfaces.—The results presented can be used to choose deposition conditions corresponding to the maximum film growth rate for which the surface remains smooth over the requisite length scale, W . To this end, we require that all perturbation modes with wavelengths smaller than W decay; i.e., $\omega(k) < 0$ for $k \geq 2\pi/W$. Equation 18 implies $j_{\text{eff}}(1 + \alpha_1)/(1 - j_{\text{eff}}) \leq \hat{\gamma}\alpha_1(2\pi/W)^2$ for the case of a fully supported electrolyte. In order to guide experiment, we express the stability conditions in terms of the experimentally accessible parameters (without changing additives), metal cation flux j (which is proportional to the growth rate), and additive concentration C_1^∞ . In Fig. 3 we construct a stability map for realistic growth conditions. Such a map conveniently displays the full range of stable and unstable growth conditions. While introducing additives can dramatically increase the deposition currents that can be used, the effect saturates at large additive concentrations. There exists a critical current $j^* \approx 1 - (1 + \alpha_1)/Y$ above which the additives are incapable of leveling the surface. This can be understood by incorporating the blocking effect into the second term of an effective overpotential $\eta_{\text{eff}} \equiv \eta + RT/F \ln(1 - \theta_1)$, obtained from the modified B-V equation. In order to produce large deposition fluxes, the metal cation concentration gradient ahead of the surface is large and the metal cation concentration is low. To maintain these high fluxes the overpotential must be large, such that $\eta \gg RT/F \ln(1 - \theta_1)$. This implies that the additives (represented by θ_1) are incapable of stabilizing the smooth surface.

Finally, let us relate the stability map to experiments. The surface is linearly stable at sufficiently small currents j even in the absence of additives. However, for sufficiently large j , instabilities with wavenumbers greater than $2\pi/W$ appear, implying roughening. Increasing C_1^∞ at fixed $j < j^*$ leads first to slower roughening and then to a transition from a rough to a smooth surface. This behavior

^c Doona and Stanbury²⁷ measured the equilibrium constant K_c for thiourea-cupric ion complex formation, from which we find $Y = \ln K_c$.

is consistent with experimental observations of Schilardi *et al.*⁷ which show that the dominant wavelength of the surface instability increases with increasing additive concentration up to a critical concentration beyond which the surface of the growing film remains level. Similarly, we predict that increasing the deposition flux j for a fixed additive bulk concentration C_1^∞ leads to a transition from planar to rough morphology.^d

Conclusions

We have introduced a chemically motivated continuum model for the morphological stability of surfaces during ED and the effects of additives on that stability. The ED model explicitly accounts for the electric field in the electrolyte, the metal cations and anions, the additives, and the spectator ions from the supporting electrolyte. The model for additives employed here accounts for three main chemical/physical phenomena: (i) the additives form complexes with the metal cations in the electrolyte, (ii) the additive molecules have a finite dipole moment and hence interact with inhomogeneities in the electric fields in the electrolyte, and (iii) the additives occupy sites on the surface, thereby blocking deposition of metal cations. The stability of the ED surface in the presence of additives was analyzed using perturbation theory. In the fully supported electrolyte case, we found that additives enhance leveling by making the surface stable on longer length scales and decreasing the rate at which roughness grows; our quantitative predictions for the stabilization length are in very good agreement with existing experimental observations. The additives stabilize the surface by decreasing the effective driving force for the instability. The effective driving force depends on the bulk concentration of the additives, the tendency of the additives to segregate onto the surface, the strength of complex formation, and the local additive flux; increasing the magnitude of any of these terms increases the surface stability. The tendency of the additives to segregate onto the surface is enhanced in the case of polar additives, which are attracted to the surface due to the presence of strong electric field gradients. This occurs for any bath composition. Additionally, the dipole moment of the additive may help further stabilize the surface in the case of an unsupported or partially supported electrolyte, as the polar additives also interact with the electric fields associated with surface protrusions. Under typical deposition conditions, however, we expect this effect to be small.

Leveling is promoted by increasing the concentration of the additives, the tendency for the additives to (thermodynamically) segregate to the surface, the tendency for additive-metal cation complexing, incorporation of the additives into the growing electrodeposit, and the tendency of the additives on the surface to block metal cation attachment. At a minimum, additives must be able to segregate to the surface in equilibrium and be able to block surface sites once they get there. In addition, at least one of the following must also be present: additive-metal cation complexing, additive incorporation in the growing deposit (or, equivalently, additive reduction at the surface), or a nonzero dipole moment (if the electrolyte is not fully supported). These different effects act in concert in a well-designed additive.

Much of these results can be summarized in stability maps that show under which experimental conditions a surface is stable or unstable for a given feature size (below which the surface must be flat). We have constructed such a map in metal cation flux j (*i.e.*, growth rate) and additive concentration C_1^∞ space. This map clearly shows the existence of a sharp boundary between the stable and unstable growth regimes as well as identifies conditions under which increasing the additive concentration is unable to suppress this natural instability.

^d The experiments of Schilardi *et al.*⁷ show that increasing the additive concentration leads to first decrease in roughness rather than an increase in roughness above some critical concentration. Those authors attribute this to a phase transition within an additive layer.

Acknowledgments

We thank Dr. Corbett Battaile and Dr. John Hamilton for fruitful discussions, and Sandia National Laboratories for financial support.

Princeton University assisted in meeting the publication costs of this article.

List of Symbols

C_i	concentration of species i
C_0	metal cation bulk concentration
C_1	spectator cation bulk concentration, normalized by C_0
C_1^∞	additive bulk concentration, normalized by C_0
D_i	diffusivity of species i
F	Faraday constant
h	position of the surface in the lab frame
j	dimensionless steady-state metal cation flux
j_i	flux of the species i
J_0	exchange flux density
k	initial perturbation wavenumber, in units of $1/L$
K	equilibrium additive surface adsorption constant
k_B	Boltzmann constant
K_c	equilibrium constant for additive-metal cation complex formation
k_{\max}	maximally unstable mode
k_0	neutral mode
L	thickness of the mass-transfer layer
ℓ_s	stabilization length
\hat{n}	surface normal, pointing into the solution
p	strength of the dipole moment per additive
$q_i e$	charge of the species i
R	gas constant
T	temperature
V_{eq}	equilibrium potential of the metal-solution interface
V_{ext}	electric potential of the metal-solution interface during growth
v_n	normal velocity of the growth front
z	distance from the surface
Greek	
β	dimensionless equilibrium potential of the metal-solution interface
γ	surface tension of the metal-solution interface
$\hat{\gamma}$	dimensionless surface tension of the metal-solution interface
Δ	dimensionless additive dipole moment
δC_i	perturbation of the species i
δj	perturbation of the local metal cation flux
$\delta \xi$	initial surface perturbation amplitude
ϵ	dimensionless thickness of the G-C boundary layer
$\hat{\epsilon}$	permittivity of the solution
η	overpotential
θ_1	additive surface coverage
κ	local curvature of the metal-solution interface
λ_{GC}	thickness of the G-C boundary layer
Υ	dimensionless strength of complex formation
ϕ	electric potential
ϕ^*	potential of the metal-solution interface, normalized by the equilibrium potential
χ	parameter describing the extent of additive codeposition
ψ	parameter which describes the strength of complexing
Ω	atomic volume of the metal in the deposit
Ω'	dimensionless atomic volume of the metal in the deposit
$\omega(k)$	growth rate of perturbation with wavenumber k

References

1. J. W. Dini, *Electrodeposition: The Materials Science of Coatings and Substrates*, Noyes Publications, Park Ridge, NJ (1993).
2. J. Oniciu and L. Muresan, *J. Appl. Electrochem.*, **21**, 565 (1991); T. C. Franklin, *Surf. Coat. Technol.*, **30**, 415 (1987).
3. F. Argoul, A. Arnedo, G. Grasseau, and H. L. Swinney, *Phys. Rev. Lett.*, **61**, 2558 (1988).
4. G. L. M. K. S. Kahanda, X.-Q. Zou, R. Farrell, and P.-O. Wong, *Phys. Rev. Lett.*, **68**, 3741 (1992).
5. D. Barkey, F. Oberholtzer, and Q. Wu, *Phys. Rev. Lett.*, **75**, 2980 (1995).
6. J. M. Pastor and M. A. Rubio, *Phys. Rev. Lett.*, **76**, 1848 (1996).
7. P. L. Schilardi, O. Azzoni, and R. C. Salvarezza, *Phys. Rev. B*, **62**, 13098 (2000).
8. D. Kandel and E. Kaxiras, *Solid State Phys.*, **54**, 219 (2000).
9. M. Haataja, D. J. Srolovitz, and A. B. Bocarsly, *J. Electrochem. Soc.*, **150**, C699 (2003).
10. M. Haataja and D. J. Srolovitz, *Phys. Rev. Lett.*, **89**, 215509 (2002).
11. C. Madore, M. Matlosz, and D. Landolt, *J. Electrochem. Soc.*, **143**, 3927 (1996).
12. M. Georgiadou, D. Veyret, R. L. Sani, and R. C. Alkire, *J. Electrochem. Soc.*, **148**, C54 (2001).
13. Y. Cao, P. Taephaisitphongse, R. Chalupa, and A. C. West, *J. Electrochem. Soc.*, **148**, C466 (2001).

14. T. J. Pricer, M. J. Kushner, and R. C. Alkire, *J. Electrochem. Soc.*, **149**, C406 (2002).
15. D. Josell, D. Wheeler, W. H. Huber, and T. P. Moffat, *Phys. Rev. Lett.*, **87**, 016102 (2001).
16. D. Josell, B. Baker, C. Witt, D. Wheeler, and T. P. Moffat, *J. Electrochem. Soc.*, **149**, C637 (2002).
17. J. D. Jackson, *Classical Electrodynamics*, John Wiley & Sons, New York (1975).
18. M. Paunovic and M. Schlesinger, *Fundamentals of Electrochemical Deposition*, John Wiley & Sons, New York (1998).
19. M. D. Pritzker and T. Z. Fahidy, *Electrochim. Acta*, **37**, 103 (1992).
20. R. Aogaki, K. Kitazawa, Y. Kose, and K. Fueki, *Electrochim. Acta*, **25**, 965 (1980).
21. D. P. Barkey, R. H. Muller, and C. W. Tobias, *J. Electrochem. Soc.*, **136**, 2207 (1989).
22. C.-P. Chen and J. Jorne, *J. Electrochem. Soc.*, **138**, 3305 (1991).
23. L.-G. Sundstrom and F. H. Bark, *Electrochim. Acta*, **40**, 599 (1995).
24. J. Elezgaray, C. Léger, and F. Argoul, *J. Electrochem. Soc.*, **145**, 2016 (1998).
25. R. Cuerno and M. Castro, *Phys. Rev. Lett.*, **87**, 236103 (2001).
26. C. H. P. Lupis, *Chemical Thermodynamics of Materials*, North-Holland, New York (1983).
27. C. J. Doona and D. M. Stanbury, *Inorg. Chem.*, **35**, 3210 (1996).